

Modular Multilevel DC Cascaded Converter with Battery Electrical Storage Integration

Gagić, Mladen; Huang, Kewei; Qin, Zian; Ferreira, Bram

DOI

[10.1109/APEC.2019.8721863](https://doi.org/10.1109/APEC.2019.8721863)

Publication date

2019

Document Version

Final published version

Published in

2019 IEEE Applied Power Electronics Conference and Exposition (APEC)

Citation (APA)

Gagić, M., Huang, K., Qin, Z., & Ferreira, B. (2019). Modular Multilevel DC Cascaded Converter with Battery Electrical Storage Integration. In *2019 IEEE Applied Power Electronics Conference and Exposition (APEC)* (pp. 182-187). Article 8721863 IEEE. <https://doi.org/10.1109/APEC.2019.8721863>

Important note

To cite this publication, please use the final published version (if applicable).
Please check the document version above.

Copyright

Other than for strictly personal use, it is not permitted to download, forward or distribute the text or part of it, without the consent of the author(s) and/or copyright holder(s), unless the work is under an open content license such as Creative Commons.

Takedown policy

Please contact us and provide details if you believe this document breaches copyrights.
We will remove access to the work immediately and investigate your claim.

Modular Multilevel DC Cascaded Converter with Battery Electrical Storage Integration

Mladen Gagic, Kewei Huang, Zian Qin, Braham Ferreira
Electrical Sustainable Energy
Delft University Of Technology
Delft, the Netherlands
m.gagic@tudelft.nl

Abstract— Medium voltage dc microgrids seeks to compete with conventional ac systems by providing various benefits regarding electrical power availability and efficiency. One method of achieving this goal is to provide a more effective and reliable interface to renewable energy sources and especially electrical storage devices. This paper presents a multilevel, cascaded converter topology that allows for the integration of various low voltage power sources and storage units into a single string of series connected half-bridge submodules. The resulting topology allows the system to function as medium-voltage dc voltage source. By implementing an additional, nested current loop, guided by passive tuned filters, the converter controls the power flow between the submodules and the system, thus achieving power balance in all operating modes. This paper presents the underlying converter control principle for configurations containing electrical battery interfacing devices. Simulation and experimental results from a scaled prototype demonstrate the converters capabilities for a wide range of output power delivery.

Keywords— multifrequency, multifunctionality, cascade, multilevel, tuned-filter, energy storage

I. INTRODUCTION

To meet the growing challenges of integrating various renewable energy sources closer to the consumer level of the energy system, researchers and engineers are exploring, and occasionally implementing electrical energy microgrids that operate primarily on a dc voltage. This shift from conventional ac systems is primarily due to the various benefits regarding efficiency, control and the inherent dc properties of the various electrical sources, loads and energy storage units that are widely available [3]. For these reasons, along with the expected further proliferation of renewable energy systems, there is a major focus on exploring and presenting various methods of providing a stable and robust dc based power system.

However, a major dilemma for any system designer is the choice regarding the value of the dc bus voltage. Namely, depending on the design and nature of the dc system in question, various commonly available electrical devices may prefer a different voltage from that which is available on any given main dc bus. As a result, various optimization strategies must confront and balance the needs of the available hardware components, grid codes and the requirements related to system expansion.

A feasible solution to these issues could potentially lay in the implementation of a modular, multilevel design, that incorporates different voltage levels into a single converter topology. These types of converters are most often found in ac systems, as they provide the various benefits regarding the

reduction of EMI, increased system redundancy and most notable for this paper, integration of additional power sources on the modules [5-8]. Thus far, these types of cascaded systems were implemented primarily to interface either exclusively photovoltaic (PV), battery storage (BES) or electrical load modules to an ac system. The various energy balancing and power delivery control schemes have, as of yet, not dealt with the proper integration of a single-arm cascaded topology for energy storage integration of different voltage levels.

This paper presents a novel application of a cascaded modular, multilevel DC converter topology with integrated BES modules. The converter is set as a dc voltage source while increasing its applicability and compatibility with dc devices of various voltage ratings using a multilevel design. To achieve a greater degree of power flow control, the converter implements an additional ac current loop inclosed within the converter and guided by passive tuned band-pass filters. This paper begins by presenting a general model of the converter along with its principles of operation in section II. The following, third section III explains the voltage source mode of operation with regards to the utilization of electrical storage devices for single-arm, multi-arm and varied voltage rating modes. Simulation and experimental results on a single string converter model are given in section IV.

II. MODULAR MULTILEVEL DC CONVERTER

The bases of the Modular Multilevel DC Converter (M2DC) represents a topologically equal first discussed in [1] and then further demonstrated in [2-3]. These types of converters operate on the same principles, which relies on the implementation of secondary (nested) current loop that circulates within the converter and provides an additional degree of power flow control [1]. The major difference, in comparison with the work presented in [2-3], is the previously mentioned integration of battery energy storages to the converters submodules (SMs) under different configurations, along with the modifications to the required controls. Whereas the initial M2DC is implemented as a single-source bidirectional step-up or step-down dc/dc converter, the integration of additional devices to the submodules has not yet been explored or tested, thus giving it its multifunctional feature.

Fig. 1 shows the topology of a single string, two-arm M2DC converter that implements a tuned passive LC filter for the guidance of the secondary current. In general, this tuned passive filter can be replaced either by an active filter or an additional converter leg [4-5]. An arm inductance divides the string leg into N upper submodules and M lower SMs. The assumption is that the submodules of each arm are interfacing either battery storage units or are left open (conventional SM). For cases in which the energy storage units in each of the arms are of a different power or voltage

rating, the underlying control mechanism needs only slight modification that will be covered by this paper. The system parameters are defined in table I.

Due to its implementation in dc systems, the M2DC possesses an additional advantage in comparison with similar cascaded ac topologies [2]. One such advantage is the previously mentioned implementation of a half-bridge SM design, which is sufficient enough for the power exchange operation with lower-voltage devices. Since the focus of this paper is on the overall converter and its control, all the BES units are considered to be connected directly to their respective SMs. A real-world application would incorporate a design which includes the proper isolation, EMI and necessary protection devices. These devices represent ready-made and widely available converters and components, rated for the appropriate voltage and current. In that regard, the system designer has a greater degree of voltage ranges to choose from, allowing for a greater integration of components with different nominal dc voltage values.

TABLE I
PARAMETERS OF THE M2DC CIRCUIT MODEL [2]

Symbols	Descriptions
V_o	Output dc voltage
I_o	Output dc current
L_{bp}	Band pass filter inductor
C_{bp}	Band pass filter capacitor
R_{arm_u}	Equivalent upper arm resistance (sum of upper arm inductor resistance and switch turn on resistance)
R_{arm_l}	Equivalent lower arm resistance (sum of lower arm inductor resistance and switch turn on resistance)
L_{arm_u}	Upper arm inductor
L_{arm_l}	Lower arm inductor
L_o	Output inductor
V_{cu}	Sum of upper arm capacitor voltage
V_{cl}	Sum of lower arm capacitor voltage
v_u	Inserted voltage of upper arm submodules
v_l	Inserted voltage of lower arm submodules
i_{sec}	Secondary current--circulating current of the secondary power loop

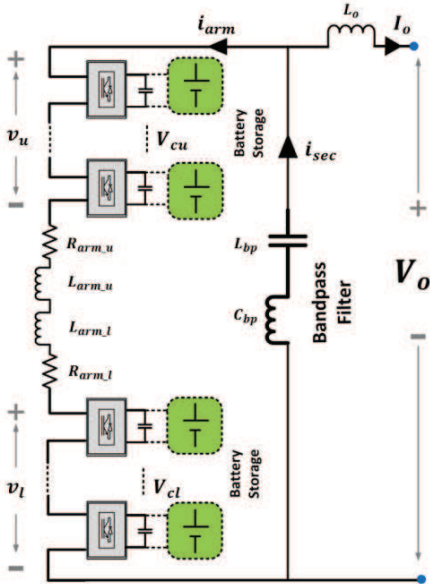


Figure 1: Modular Multilevel Cascaded DC Converter with Battery-Electrical Storage Integration.

The basic control principle of the M2DC relies on two modes of operation, inductive coupled mode (ICM) in which the converter behaves as a current source, and resistive coupled mode (RCM), for which the system operates as a voltage source across its main terminals [2]. For this paper, the converter operates in the RCM, since it is more applicable to the requirements of dc microgrid systems and allows for a greater degree of control.

A more in-depth description of a single string, tuned-filter M2DC is found in [2]. The converter controls all submodules via their respective arm. Similar to the conventional methods of modulation deploy in standard modular multilevel converters (MMC), the injected voltage references of the upper and lower converter arm are represented by (1) and (2) for the upper and lower arm respectively. Unlike their ac/dc converter counterpart, the goal of the M2DC is not to nullify the dc component, but to implement it while nullifying the ac voltage from the main terminal. Therefore, there is a greater utilisation of both the dc and ac reference values, as will be evident later on in the paper. The PWM carrier signals of the controller utilized the phase-shift method for the individual submodules.

$$u_{ref_u} = D_u - m_u \cdot \cos(\omega t + \varphi) \quad (1)$$

$$u_{ref_l} = D_l + m_l \cdot \cos(\omega t) \quad (2)$$

The secondary (nested) current is key to the proper operation of the converter. In the case of the resistive-coupled mode of operation, the generated upper and lower SM ac voltages define the circulating current (3).

$$i_{sec} = \frac{V_{cu} \cdot m_u - V_{cl} \cdot m_l}{R_{arm_u} + R_{arm_l}} \cdot \cos(\omega t) \quad (3)$$

Depending on the mode of operation, apart from the secondary current, the converter arm may also contain a dc current component I_o . Important values for the power flow control algorithms presented in the following section are the mean powers of the upper and lower submodules, presented by (4) and (5). These equations are obtained by multiplying the arm currents with the respective injected lower or upper arm voltages. By integrating these instantaneous powers for a period defined by the secondary current, the mean powers of the upper and lower submodules are thus obtained.

$$P_u = -V_{cu} \cdot D_u \cdot I_o - \frac{V_{cu} \cdot m_u - V_{cl} \cdot m_l}{R_{arm_u} + R_{arm_l}} \cdot \frac{V_{cu} \cdot m_u}{2} \quad (4)$$

$$P_l = V_{cl} \cdot D_l \cdot (I_{in} - I_o) + \frac{V_{cu} \cdot m_u - V_{cl} \cdot m_l}{R_{arm_u} + R_{arm_l}} \cdot \frac{V_{cl} \cdot m_l}{2} \quad (5)$$

In the inter-terminal version of the M2DC [], the mean power would be equal to zero. However, in the case of the configuration presented in this paper, the mean power of each converter arm is dependant on power exchange on three different levels:

1. Electrical power injected or absorbed by the submodules.
2. Power exchange between the upper and lower arm.
3. Power transfer with the main terminal.

The first level of power exchange primarily depends on the type of device interfacing the submodule. Electrical

power sources, loads, energy storage and even non-interfacing submodules are all applicable in the M2DC.

For the second level of power exchange, the amount of power transferred between the two converter arms is dependent on both the converter mode of operation, as well as the control parameter that will be addressed in the following section.

The third level of power exchange accounts for any amount of power delivered to the main terminal (dc grid) as a result of the dc voltage source operation.

III. POWER EXCHANGE CONTROL BY MEANS OF SECONDARY POWER LOOPS

To achieve a stable dc voltage across the converter terminals, the converter needs to utilize the two pairs of parameters for the upper and lower submodules. Depending on the converter application, two main configurations are presented:

1. Single-arm storage configuration.
2. Dual-arm interconnection of el. storage.

Since the converter submodules are a half-bridge topology, they are capable of only delivering dc power when the converter is set as a voltage source. This power is determined by the dc current component of the arm, as well as the dc component of the injected arm voltage. Therefore, this represents the dc power delivered to the grid terminals. By contrast, the power exchange between the modules is achieved via the circulating current. By observing (4) and (5), it is evident that to maintain a power balance, (6) needs to be satisfied. Therefore, the ac reference voltage injection plays a key role in both specifying the converter arm voltage (under the first configuration) and determining the amount of second-level power transfer for the second configuration.

$$m_u \cdot V_{cu} = m_l \cdot V_{cl} \quad (6)$$

A. Single-Arm Storage Configuration

The single-arm storage configuration implies that electrical storage units are connected only to either the upper or lower converter arm. Likewise, this work assumes that all the converter submodules are of identical design and that the energy storage units are of equal voltage ratings. For the analysis presented in this paper, it is assumed that the lower converter arms are interfaced to energy storage devices, while the upper converter arm comprises several submodules that do not interface to any device.

Two distinct cases for this configuration are observed:

- The converter output voltage is lower than the half the sum of lower arm capacitor voltage.
- The converter output voltage greater than the half lower converter arm capacitor voltage sum.

For this configuration, the control parameter diagram is given in Fig. 2. Set the dc voltage injection reference value of both converter arm to 0.5. After establishing the required output voltage, determine which of the previous two cases is applicable. It is assumed that the capacitor voltages of the lower (storage interfacing arm) are being measured.

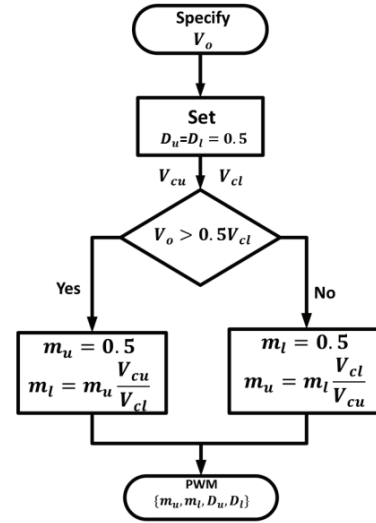


Figure 2: Control Flow Diagram of M2DC Single-arm Configuration

The method for achieving the required voltage is relatively straightforward. In the first case, set the lower arm ac voltage injection value to 0.5. To increase the voltage of the upper converter arm, implement (6) to determine the required upper arm ac injected voltage reference. In the second case, where a lower voltage is required, the opposite steps must be undertaken. Therefore, the upper arm m_u parameter is set to 0.5, while the lower arm parameter is lowered, based on equation (6).

B. Dual-Arm Interconnection of Electrical Storage

In the second configuration, both the lower and upper converter arms are now interfaced to various types of electrical storage devices via the submodules. For this configuration, all three levels of power flow control need to be taken into account. As previously mentioned, the two converter arms may differ in the sum of their respective capacitor voltages, all of which are assumed to be tracked. The converter output voltage is now determined by the aforementioned upper and lower arm capacitor voltage sum and their respective dc voltage injection reference.

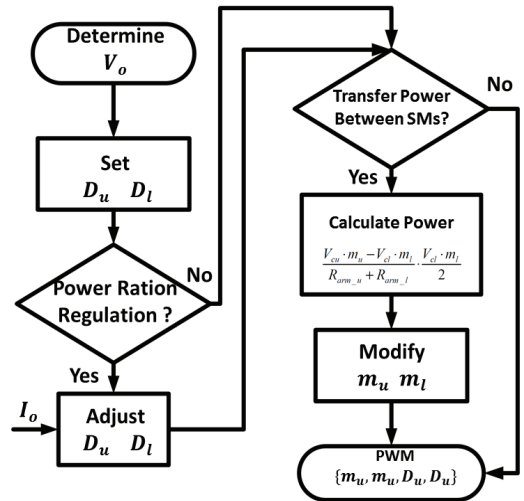


Figure 3: Control Flow Diagram of M2DC Dual-arm Configuration.

Taking into account the three levels of converter power flow, two degrees of power flow control needs to be taken into consideration. Firstly is the dc power that the submodules inject into the arm. This power is determined by the arm dc current component as well as the dc voltage injection. If the storage rate of discharge is of concern to the system designer, then this dc current must be tracked and the dc injection voltage adjusted. The second degree of power flow allows the converter to directly share energy between the two submodules via the secondary current. Namely, by utilizing the second component of (4) and (5), the ac voltage injection references can be set (with prior knowledge of the capacitor sum voltages) to transfer a certain amount of power from one converter arm to the other.

Control flow for this mode of operation is shown in Fig. 3. Assuming that all the capacitor voltages are tracked, the initial step is to specify the dc voltage injection ratios. In case the discharge rate control of the el. energy storage units is required, the output current needs to be measured and the dc reference adjusted accordingly. The following step involves the second level of power flow control. Based on the measured capacitor voltages and the knowledge of the coupling arm resistance, (4) and (5) should be utilized to specify the direction and amount of power transferred between the converter arms. If not, (6) should be satisfied.

IV. SIMULATION AND EXPERIMENTAL RESULTS

This section contains the simulation and experimental results for the two M2DC configuration and their variants. The basic control principles underlined in the previous section have been tested in open-loop on a simulation model as well as on a scaled hardware prototype. Both the model and the experimental setup schematics are featured in Fig. 4 with the relevant parameters in table II. As is visible, the M2DC converter consisting of four submodules (two on each arm), with the two on the top being either non-interfacing or interfaced to a higher dc voltage than the remaining lower two energy storage units.

The simulations were carried-out via *Matlab Simulink*. Voltage source blocks are placed on each of the two upper arm submodules in place of a battery unit, while the output terminal is connected to a resistor block.

For the experimental setup, shown in Fig. 5, the submodules are each interfaced to a bidirectional Delta Electronics SM500-CP-90 bidirectional power supply standing-in for either as a 24V or 30V dc battery replacement. Finally, a variable passive-resistor across the output terminals was implemented for the voltage source experiments.

A. Single-arm storage configuration results.

When the converter is configured to operate with BES on only one (in the case this paper, the lower) converter arm, the mechanism for second-level power transfer relies on the circulating ac current. Namely, for the converter to provide a fixed dc voltage across its terminals, the voltage across the upper arm SM capacitors needs to be maintained. As was specified in section III.A, the converter submodule ac voltage injection references are utilized to vary, and therefore adjust the overall voltage across the main terminal.

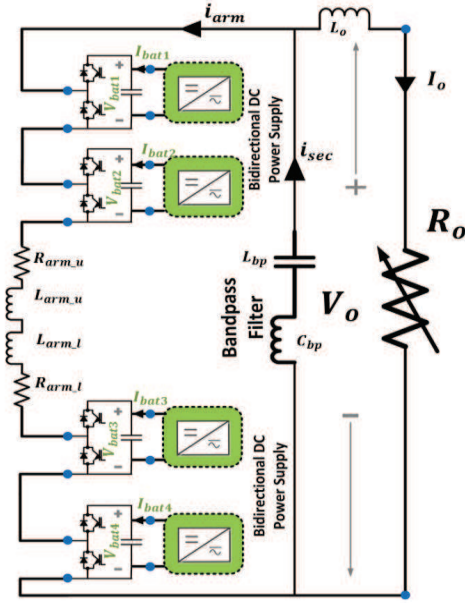


Figure 4: Simulation and Experimental M2DC Schematic.

TABLE II
PARAMETERS OF THE M2DC CONVERTER [2]

Parameters	Values
Secondary frequency	1.953 KHz
Switching frequency	24.4 KHz
Band pass filter inductance	98 μ H
Band pass filter inductor resistance	34 m Ω
Band pass filter capacitance	67.7 μ F
Output inductance	2894 μ H
Output inductor resistance	333 m Ω
Arm inductance of RCM	9.35 μ H
Arm inductor resistance of RCM	14 m Ω
Capacitance of SM_{u1}	199 μ F
Capacitance of SM_{u2}	200 μ F
Capacitance of SM_{l1}	202 μ F
Capacitance of SM_{l2}	203 μ F
Turn on resistance of IRFB4127PbF	17 m Ω
Snubber resistance	0.25 Ω
Snubber capacitance	2 nF

Fig. 6 depicts the simulation results for a fixed output load resistance. The upper submodule voltage capacitance (Fig. 6.a) is increased by means of decreasing the ac voltage injection reference of the upper submodules (Fig. 6.b). As is evident, the voltage increases fairly linearly with the reference signal. Likewise, the converter circulating current in Fig. 6.c gradually increases as a result of the ac power transfer. This ac power is then converted to the upper SM injected dc power.

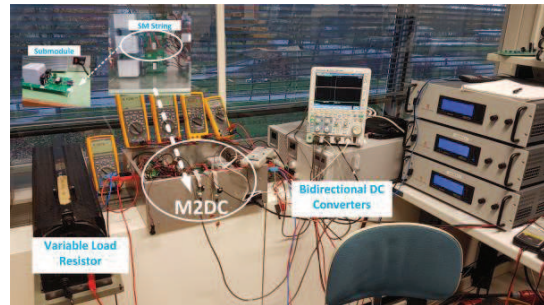


Figure 5: M2DC Experimental Prototype Setup.

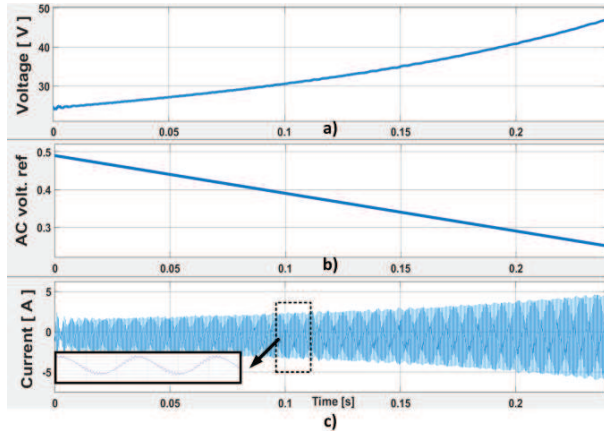


Figure 6: Increasing upper SM capacitor voltage simulation results for single-arm configuration M2DC interfacing a fixed 90Ω load.
 $(D_l = D_u = 0.5; m_l = 0.5; V_{cu} = 48V)$

In contrast, Fig.7 shows simulation for the same operating conditions with the goal of decreasing the upper SM capacitor voltage Fig.7.a. This is accomplished by reducing the lower converter arm ac voltage injection reference Fig.7.b. The ac circulating current remains constant, since the decrease in voltage is proportional to a lower dc power injection of the upper submodule. Experimental measurements for this configuration are provided in Fig.8.

The output voltage regulation capabilities of the converter were conducted via simulation and experimentation for an output voltage set to 48V, with the results depicted in Fig.9. With an incremental lowering of the load resistance across the terminal the converter delivers more dc power. The simulation results depict that the output voltage experiences a gradual deviation from its nominal value. This can be attributed to an increasing voltage drop between the submodule string and the output terminals. The voltage deviation is greater in the experimental results with increased output currents. This is also partly attributed to the voltage drift of the upper submodules as a result of insufficient voltage balancing.

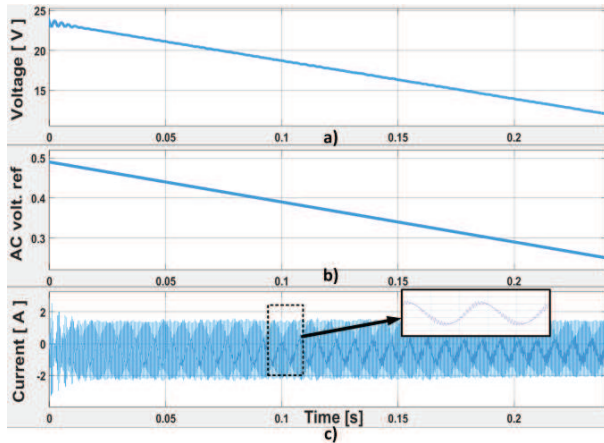


Figure 7: Decreasing upper SM capacitor voltage simulation results for single-arm configuration M2DC interfacing a fixed 90Ω load.
 $(D_l = D_u = 0.5; m_u = 0.5)$

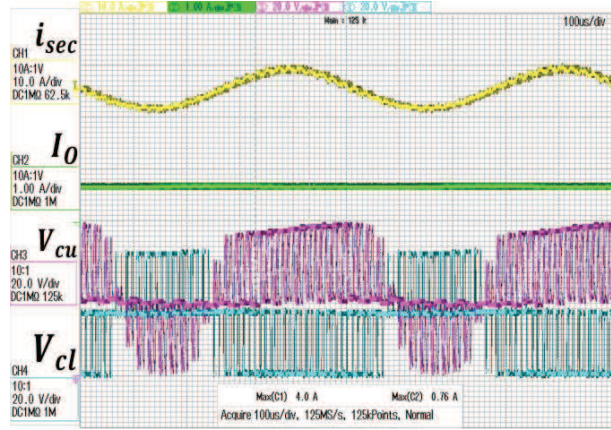


Figure 8: Experimental measurements for single-arm configuration M2DC
 $(D_l = D_u = 0.5; m_l = m_u = 0.5; V_{cu} = 48V; R_o = 90\Omega)$

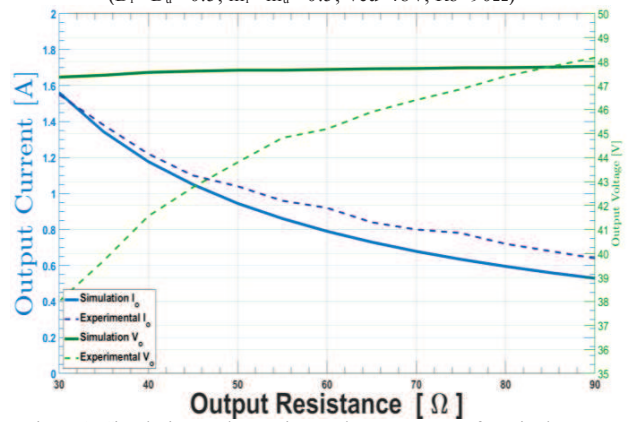


Figure 9: Simulation and experimental measurement for single-arm configuration M2DC $(D_l = D_u = 0.5; m_l = m_u = 0.5; V_{cu} = 48V; R_o: \text{variable})$

B. Dual-arm interconnection of electrical storage experiments

When the upper and lower converter arm is interfacing electrical storage units of different nominal voltages, the balancing of (4) and (6) is crucial for the ac circulating current control. For this case, the simulations and experiments were conducted with two 24V BES on the lower two and 30V units on the upper two submodules. A fixed resistance of 90Ω is placed across the terminals for the simulations conducted and depicted in Fig.10 and Fig.11

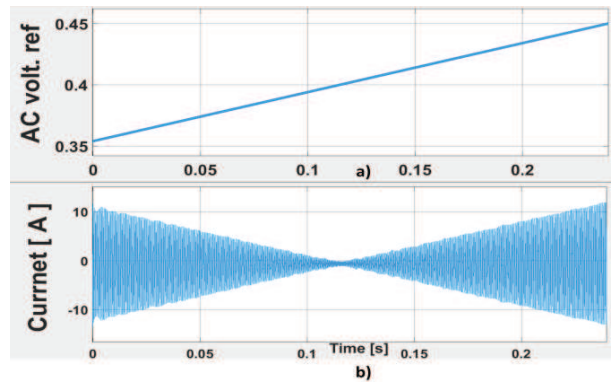


Figure 10: Simulation results for dual-arm configuration M2DC interfacing a fixed 90Ω load while varying injected ac voltage of upper arm.
 $(D_l = D_u = 0.5; V_{cu} = 48V; V_{cl} = 60V; m_l = 0.5; m_u: \text{variable})$

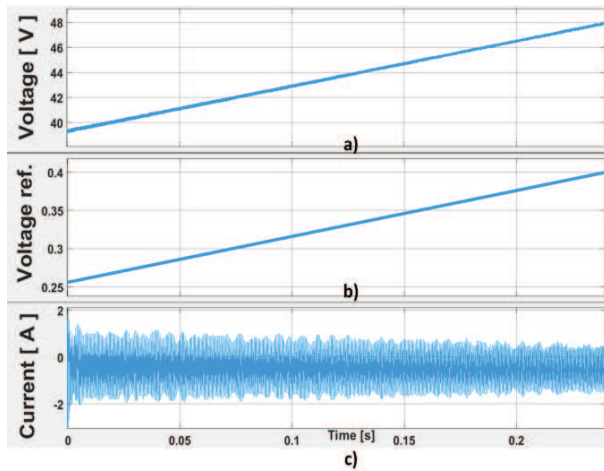


Figure 11: Simulation results for dual-arm configuration M2DC interfacing a fixed 90Ω load while varying injected ac voltage of upper arm.

($D_f = 0.5$; $V_{cu} = 48V$; $V_{cl} = 60V$; m_f : varying $D_u = m_u$: variable)

Fig.10.b demonstrates the change in the circulating current when the upper arm ac voltage injection reference is altered around a balanced operating point Fig.10.a. At the lowest current value, there is a minimum second level power transfer between the converter arms. Likewise, on either sides of this point the BES devices on opposite converter arms exchange power with each other.

In Fig.11 the dc and ac voltage injection references of the upper converter arm are adjusted in tandem with the lower arm ac reference to increase the output terminal voltage Fig.11.a.

Measurements from this experimental equivalent are given by Fig.12. Fig.13 depicts the measured output current and voltage for a varying output load in the configuration stated earlier. Unlike the single-arm configuration, the output voltage is more uniform, owing to the fact that the submodule capacitor voltages are more stable as a result of a direct connection with 30V electrical storage devices.

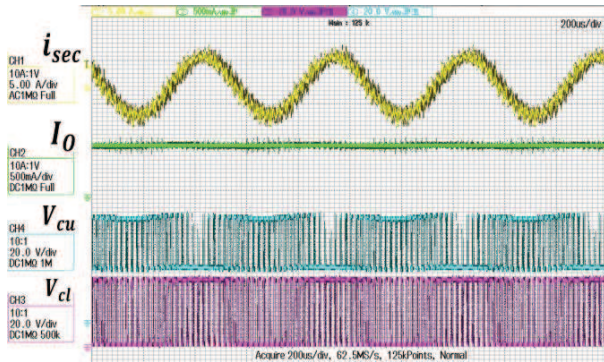


Figure 12: Experimental measurements for dual-arm configuration M2DC ($D_f = D_u = 0.5$; $m_f = 0.5$; $m_u = 0.385$; $V_{cu} = 48V$; $V_{cl} = 60V$; $R_o = 90\Omega$)

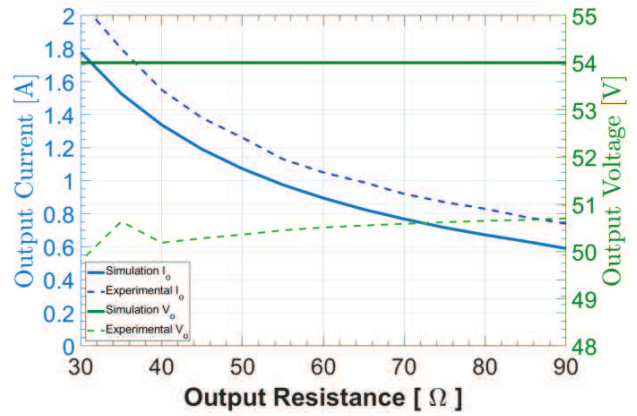


Figure 13: Experimental measurement for dual-arm configuration M2DC ($D_f = D_u = 0.5$; $m_f = 0.5$; $m_u = 0.385$; $V_{cu} = 48V$; $V_{cl} = 60V$; R_o : variable)

V. CONCLUSION

The Modular Multilevel DC Cascaded Converter provides various benefits to applications that require a greater degree of flexibility, robustness and voltage levels. By utilizing the multilevel feature of its design, the M2DC is capable of integrating a larger number and variation of electrical storage devices. A secondary, nested ac circulating current of a specified frequency allows for a single converter string configuration with direct dc voltage terminals.

REFERENCES

- [1] J. A. Ferreira, "The Multilevel Modular DC Converter," in *IEEE Transactions on Power Electronics*, vol. 28, no. 10, pp. 4460-4465, Oct. 2013. doi: 10.1109/TPEL.2012.2237413
- [2] K. Huang and J. A. Ferreira, "Two operational modes of the modular multilevel DC converter," *2015 9th International Conference on Power Electronics and ECCE Asia (ICPE-ECCE Asia)*, Seoul, 2015, pp. 1347-1354. doi: 10.1109/ICPE.2015.7167954.
- [3] J. P. Barton and D. G. Infield, "Energy storage and its use with intermittent renewable energy," in *IEEE Transactions on Energy Conversion*, vol. 19, no. 2, pp. 441-448, June 2004. doi: 10.1109/TEC.2003.822305
- [4] Y. Li, F. Gruson, P. Delarue and P. Le Moigne, "Design and control of modular multilevel DC converter (M2DC)," *2017 19th European Conference on Power Electronics and Applications (EPE'17 ECCE Europe)*, Warsaw, 2017, pp. P.1-P.10.
- [5] H. Yang and M. Saeedifard, "Closed-loop control of the DC-DC modular multilevel converter," *2016 IEEE Energy Conversion Congress and Exposition (ECCE)*, Milwaukee, WI, 2016, pp. 1-8. doi: 10.1109/ECCE.2016.7854920
- [6] M. Vasiladiotis and A. Rufer, "Balancing control actions for cascaded H-bridge converters with integrated battery energy storage," *2013 15th Eur. Conf. Power Electron. Appl. EPE 2013*, vol. 1, 2013
- [7] F. Gao, L. Zhang, Q. Zhou, and M. Chen, "State-of-Charge Balancing Control Strategy of Battery Energy Storage System Based on Modular Multilevel Converter," *IEEE Energy Convers. Congr. Expo.*, pp. 2567-2574, 2014
- [8] H. Zhou, T. Bhattacharya, D. Tran, T. S. T. Siew, and A. M. Khambadkone, "Composite energy storage system involving battery and ultracapacitor with dynamic energy management in microgrid applications," *IEEE Trans. Power Electron.*, vol. 26, no. 3, pp. 923-930, 2011